

**LATITUDINAL VARIATION IN MERCURY'S REFLECTANCE FROM THE MERCURY LASER ALTIMETER.** G. A. Neumann<sup>1</sup>, X. Sun<sup>1</sup>, E. Mazarico<sup>1</sup>, A. N. Deutsch<sup>2</sup>, J. W. Head<sup>2</sup>, D. A. Paige<sup>3</sup>, L. Rubanenko<sup>3</sup>, H.C.M. Susorney<sup>4</sup>, <sup>1</sup>NASA Goddard Space Flight Center, Greenbelt, MD 20771, (gregory.a.neumann@nasa.gov), <sup>2</sup>Brown University, Providence, RI 02912, USA, <sup>3</sup>UCLA, Los Angeles, CA 90095, USA, <sup>4</sup>Johns Hopkins University, Baltimore, MD 21219, USA.

**Introduction:** The Mercury Laser Altimeter (MLA) measured reflectivity at zero phase angle, producing a photometrically uniform data set at 1064 nm wavelength over the northern hemisphere, even in areas of permanent shadow. Surface reflectances  $r_s$  [1] of permanently shadowed regions (PSRs) near Mercury's north pole are anomalously brighter or darker than average, interpreted as evidence of water ice and other volatiles [2, 3]. Reflectance measurements were corroborated by images showing distinctive properties attributed to volatile deposits within PSR regions using scattered light [4]. These exposures are closely associated with but more extensive than the areas of high radar backscatter in the north polar region [5] interpreted as near-surface water ice, and also are seen where no radar signature has been detected [6]. The reflectance data shown here also suggests that a more widespread distribution of volatiles exists outside of PSRs, which may result from the presence of ubiquitous micro-cold traps at latitudes greater than 75°N [Rubanenko et al., this meeting].

We present a map of reflectance (Fig. 1) that has been empirically re-calibrated to mitigate biases arising from the more-than-hundredfold variation in signal return energy, incidence/emission angles varying from 0° (nadir) to 60°, and the progressive aging of the MLA instrument over four years of operation.

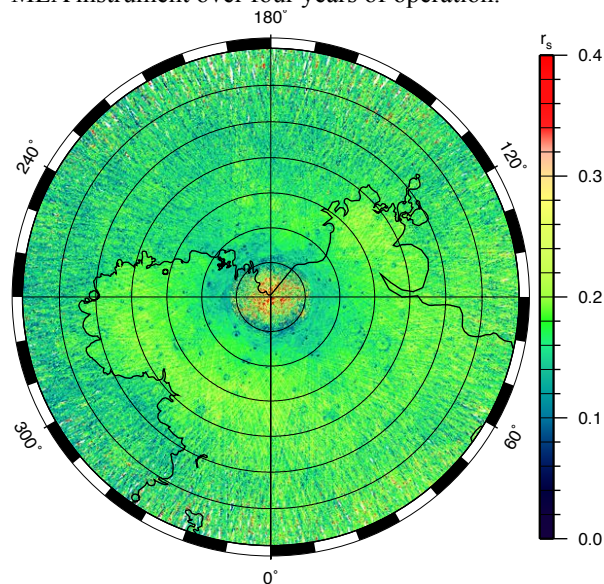


Figure 1. MLA zero-phase reflectance from four years of data 2011–2015, with outline of the mapped extent of the northern smooth plains [7]. Polar stereographic projection 55°N to pole.

To compensate for the progressive decline in MLA effective range over four mission years, as well as the effects of range, emission angle, and laser beam divergence on the width of the returned laser pulses, we estimated an average pulsewidth for each return. Broadened pulses show a characteristic downwards bias in the energy estimated from the link equation and the lidar electronics [1]. We scaled reflectances by a factor ranging from unity to a factor of two, using an arctangent response function of predicted pulse width, and excluded ranges shorter than 100 km and emission angles >50°. As the MLA laser aged, its beam divergence angle widened, contributing to a decline in signal received within the field of view of the detector. We empirically corrected for the decline in signal as a function of time using a cubic polynomial that balances the response at mid-latitudes.

**Latitudinal Averages:** The resulting MLA map shows 10–20% higher reflectance over the northern smooth plains [9], including some highly resurfaced basins such as Henri (80°N, 153°E). To explore latitudinal dependence poleward of 40°N, where the density of observations is highest owing to the eccentric MESSENGER trajectory, we averaged the reflectance in 0.25-degree intervals of latitude (Fig. 2, dashed curve). The average increases northward of ~60°N, and reaches a maximum at 72°N, after which it begins to decline, reaching a minimum at 85.3°N. Poleward of this latitude (where extensive ice deposits were observed in Prokofiev Crater [1]), reflectance increases.

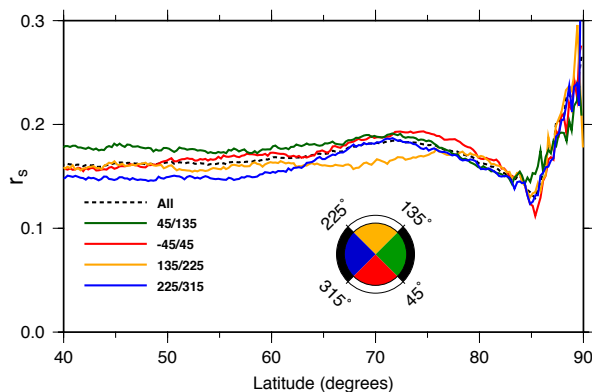


Figure 2. MLA reflectance vs. latitude at 0.25-degree intervals, averaged in quadrants to account for differences in terrain and solar illumination.

To remove the influence over these averages of large deposits within PSR craters, 190 craters of diameters

from 7-120 km were masked, as shown in Fig. 3, before averaging within quadrants.

The polar darkening continues to slightly higher latitude in the “hot longitudes”, which refer to the alternating subsolar longitudes at Mercury perihelion centered on 0°E and 180°E. The hot quadrants (red, orange) are slightly brighter from 75°N to 83°N, although there is a possible influence of the northern smooth plains distribution. The abrupt increase above 85°N is observed in all quadrants.

**Discussion:** Radar observations have suggested the presence of near-surface water ice at cold longitudes as far south as 67°, while the neutron spectrometer measurements [8] suggest near-surface hydrogen content increasing poleward of ~70°N. The earliest evidence of MLA surface ice reflectance on poleward-facing slopes is northward of 83°N [1], while dark deposits were observed coinciding with the southernmost radar features. Some poleward-facing slopes just outside of PSRs exhibit diffuse darkening above 75°N, suggesting that many small (<6 km diameter) areas of permanent shadow function as cold traps. Within these areas, both surface exposures of water ice and low-

reflectance surfaces interpreted to consist of a surficial layer of volatile organic-rich materials, formed as lag deposits, modulate the 1064-nm albedo, with a relatively rapid (10-20 km?) transition from low reflectance to high reflectance at 85.3-85.5°N. This study confirms earlier observations of MLA-bright regions, but also finds a diffuse brightening outside of the known PSR craters northward of ~85°N, corresponding to the MLA-derived and imager-derived shadowed regions [6], providing further evidence of the presence of micro-cold traps.

#### References:

- [1] M. A. Slade et al. *Science* 258 (1992), 635–638.
- [2] G. A. Neumann et al. *Science* 339 (2013), 296–300.
- [3] D. A. Paige et al. *Science* 339 (2013), 300–303.
- [4] N. L. Chabot et al. *Geology* 42 (2014), 1051–1054.
- [5] J. K. Harmon et al. *Icarus* 221 (2011), 37–50.
- [6] A. N. Deutsch et al. *Icarus* 280 (2016), 158–171.
- [7] J. W. Head et al. *Science* 333 (2011), 1853–1856.
- [8] D. J. Lawrence et al. *Science* 339 (2013), 292–296.
- [9] B. W. Denevi et al. *J. Geophys. Res.: Planets* 118 (2013), 891–907.

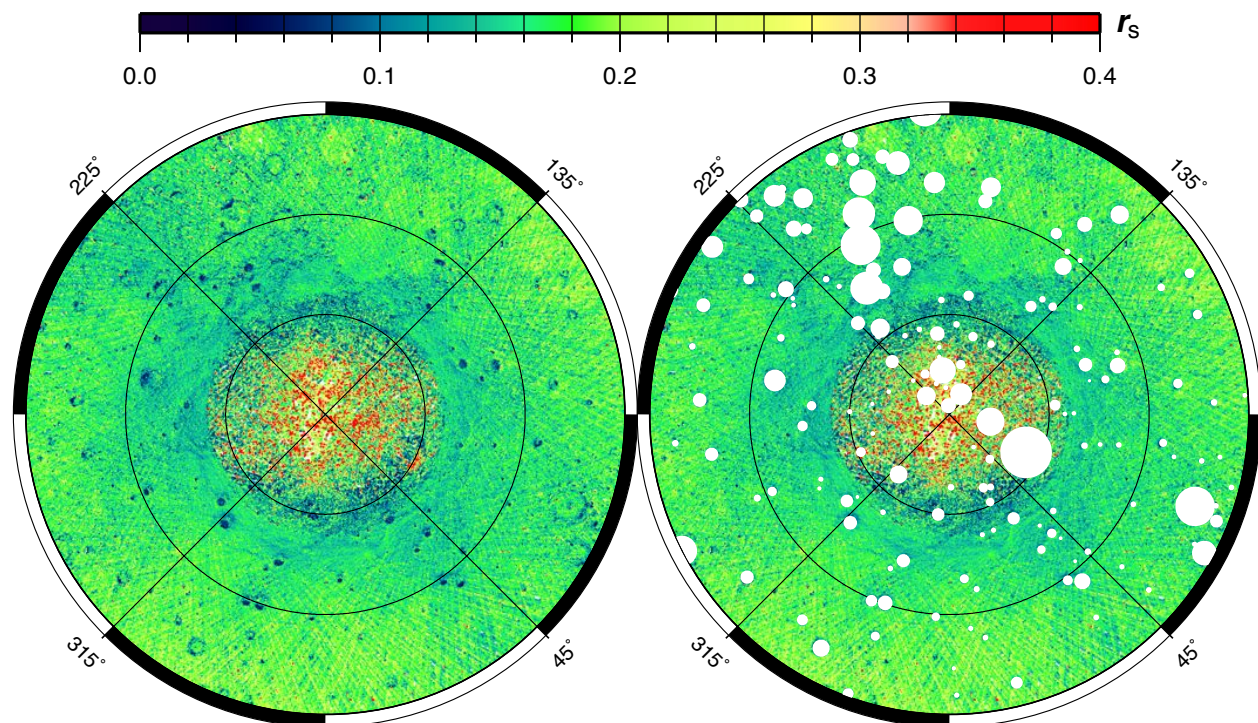


Figure 3. Reflectance in quadrants from 75°N to pole as in Figure 1, before/after removing craters containing PSRs.